

Final Report (02/01/2007-01/31/2011)

1. **DOE award #:** DE-FG02-07ER46358
Name of institution: Tulane University
2. **Project Title:** Studies of Novel Quantum Phenomena in Ruthenates
Name of the PI: Zhiqiang Mao, Professor in Physics
3. **Date of the report:** April 5, 2011
Period covered by the report: 02/01/2007--01/31/2011
4. **Participating National Laboratory:** Los Alamos National Laboratory

5. Brief description (abstract) of project goal and objective

Strongly correlated oxides have been the subject of intense study in contemporary condensed matter physics, and perovskite ruthenates $(\text{Sr,Ca})_{n+1}\text{Ru}_n\text{O}_{3n+1}$ have become a new focus in this field. One of important characteristics of ruthenates is that both lattice and orbital degrees of freedom are active and are strongly coupled to charge and spin degrees of freedom. Such a complex interplay of multiple degrees of freedom causes the properties of ruthenates to exhibit a gigantic response to external stimuli under certain circumstances. Magnetic field, pressure, and chemical composition all have been demonstrated to be effective in inducing electronic/magnetic phase transitions in ruthenates. Therefore, ruthenates are ideal candidates for searching for novel quantum phenomena through controlling external parameters. The objective of this project is to search for novel quantum phenomena in ruthenate materials using high-quality single crystals grown by the floating-zone technique, and investigate the underlying physics. The following summarizes our accomplishments.

6. Description of accomplishments

We have focused on trilayered $\text{Sr}_4\text{Ru}_3\text{O}_{10}$ and bilayered $(\text{Ca}_{1-x}\text{Sr}_x)_3\text{Ru}_2\text{O}_7$. We have succeeded in growing high-quality single crystals of these materials using the floating-zone technique and performed systematic studies on their electronic and magnetic properties through a variety of measurements, including resistivity, Hall coefficient, angle-resolved magnetoresistivity, Hall probe microscopy, and specific heat. We have also studied microscopic magnetic properties for some of these materials using neutron scattering in collaboration with Los Alamos National Laboratory. We have observed a number of unusual exotic quantum phenomena through these studies, such as an orbital selective metamagnetic transition, bulk spin valve effect, and a heavy-mass nearly ferromagnetic state with a surprisingly large Wilson ratio. Our work has also revealed underlying physics of these exotic phenomena. Exotic phenomena of correlated electron has been among central topics of contemporary condensed matter physics. Ultrafast phase transitions accompanied by switching of conductivity or magnetization in strongly correlated materials are believed to be promising in developing next generation of transistors. Our work on layered ruthenates has remarkably advanced our understanding of how the exotic phenomena of correlated electrons is governed by the complex interplay between charge, spin, lattice and orbital degrees of freedom.

In addition to studies on ruthenates, we have also expanded our research to the emerging field of Fe-based superconductors, focusing on the iron chalcogenide $\text{Fe}_{1+y}(\text{Te}_{1-x}\text{Se}_x)$ superconductor system. We first studied the superconductivity of this alloy system following the discovery of superconductivity in FeSe using polycrystalline samples. Later, we successfully grew high-quality single crystals of these materials. Using these single crystals, we have determined the magnetic structure of the parent compound Fe_{1+y}Te , observed spin resonance of superconducting state in optimally doped samples, and established a phase diagram. Our work has produced an important impact in this burgeoning field. The PI presented an invited talk on this topic at APS March meeting in 2010.

We have published 19 papers in these two areas (one in *Nature materials*, five in *Physical Review Letters*, and nine in *Physical Review B*) and submitted two (see the list of publications attached below).

6a. Orbital selective metamagnetic transition in trilayered ruthenate $\text{Sr}_4\text{Ru}_3\text{O}_{10}$

$\text{Sr}_4\text{Ru}_3\text{O}_{10}$ shows a puzzling coexistence of ferromagnetism and metamagnetism [1]. Our previous work has revealed that its metamagnetic transition occurs via an unusual electronic phase separation process [2,3]. We have clarified the origin of the coexistence of ferromagnetism and metamagnetism in this material through systematic studies of directional, angle-resolved magnetoresistivity. We find that the magnetism of this material is governed by the orbital degree of freedom: the Ru $4d_{xy}$ orbital is ferromagnetic, while Ru $4d_{xz,yz}$ orbitals are metamagnetic [4]. As far as we know, this is presumably the first example of an itinerant metamagnetic transition involving orbital selection. We have published 4 papers for this study (three in *Phys. Rev. B* and one in *J. Phys. Cond.*).

The key evidence of orbital-selective metamagnetic transition in $\text{Sr}_4\text{Ru}_3\text{O}_{10}$ is from our systematic investigations on magnetic field orientation dependences of intraplanar and interplanar magnetoresistivity ($\rho_{ab}(B, \phi, \theta)$ and $\rho_c(B, \phi, \theta)$) [4]. $\rho_{ab}(B, \phi, \theta)$ exhibits a remarkable field-dependent FM anisotropy with a twofold symmetry below the metamagnetic transition field B_c and a fourfold symmetry above B_c (see Fig. 1), whereas $\rho_c(B, \phi, \theta)$ shows a fourfold symmetry attributable to spin polarization only when the applied field is increased above B_c . In addition, we observe a giant decrease in ρ_c attributable to spin polarization when applied field is above B_c and rotated from the c axis toward the ab -plane. Since the interplanar resistivity ρ_c reflects transport properties of charge carriers from the Ru $4d_{xz,yz}$ orbitals hybridized with apical O $2p$ orbitals, while the intraplanar resistivity ρ_{ab} primarily probes charge carriers from the Ru $4d_{xy}$ orbitals hybridized with planar O $2p$ orbitals, our observations of distinct anisotropy between ρ_{ab} and ρ_c indicate that the magnetism in $\text{Sr}_4\text{Ru}_3\text{O}_{10}$ is orbital dependent, where the $d_{xz,yz}$ orbitals are responsible for the metamagnetic transition.

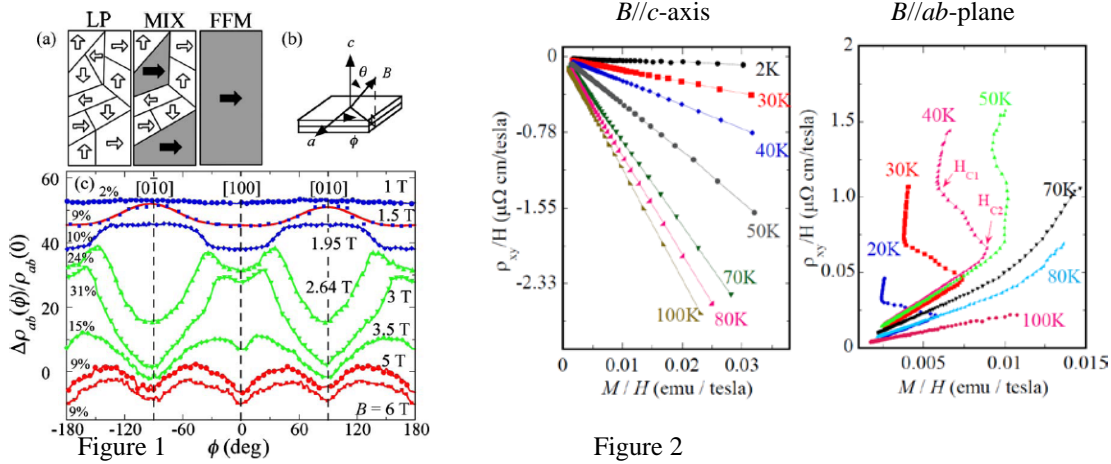


Figure 2

Figure 1: (a) Schematic representation of the three magnetic phases previously observed in $\text{Sr}_4\text{Ru}_3\text{O}_{10}$ (Refs. 2 and 3); LP, lowly polarized state; FFM, forced ferromagnetic state; MIX, mixed state). (b) Definition of polar and azimuthal angles. $\phi=0^\circ$ and $\theta=90^\circ$ is $[100]$ (a axis) and $\theta=0^\circ$ is $[001]$ (c axis). (c) Normalized azimuthal angle dependence of inplane magnetoresistivity $\Delta\rho_{ab}(\phi)/\rho_{ab}(0)$ at selected applied magnetic fields and 2 K, where $J//a$. From the top down, 1, 1.5, and 1.95 T are within the LP phase, 2.64, 3, and 3.5 T are within the mixed phase, and 5 and 6 T are within in the FFM phase. The solid curve at 1.5 T represents a theoretical fitting. The relative magnitude of anisotropy is indicated in percentage [4].

Figure 2: Hall effect of $\text{Sr}_4\text{Ru}_3\text{O}_{10}$. Left, the Hall resistivity divided by magnetic field ρ_{xy}/H vs. the magnetization divided by the field M/H at various temperatures for $B//c$. Right: ρ_{xy}/H vs. M/H at various temperatures for $B//ab$.

The orbital-selective metamagnetic transition in $\text{Sr}_4\text{Ru}_3\text{O}_{10}$ is also supported by our recent Hall coefficient measurements. For $B//c$ -axis, the Hall effect originates from in-plane transport, which primarily probes transport properties of charge carriers from Ru $4d_{xy}$ bands, while for $B//ab$ -plane the Hall effect comes from the out-of-plane transport, which should probe Ru $4d_{xz,yz}$ bands. We observe distinct Hall effects between $B//c$ and $B//ab$ -plane in the ferromagnetic state, as shown in Fig. 2. The Hall resistivity ρ_{xy} of $B//c$ follows the scaling relation with magnetization M , $\rho_{xy} = R_0H + 4\pi R_sM$, which is usually observed in ferromagnetic metals and semiconductors. However, for $B//ab$ -plane, ρ_{xy}/H exhibits a surprising dependence on M/H when the temperature is below 70 K, where metamagnetic transitions occur. The turning points indicated by arrows in the figure represent lower (H_{c1}) and upper critical fields (H_{c2}) for the metamagnetic transitions. As seen in the figure, ρ_{xy}/H vs. M/H follows linear dependence for $H < H_{c1}$ and $H > H_{c2}$, but not for $H_{c1} < H < H_{c2}$. We can extract Hall coefficient R_0 from linear fitting for both $H < H_{c1}$ and $H > H_{c2}$ ranges. R_0 is negative for $H < H_{c1}$, but becomes positive for $H > H_{c2}$; this clearly indicates that the Fermi surface pockets from the $d_{xz,yz}$ orbitals exhibit remarkable changes through the metamagnetic transition. This finding is consistent with the general expectation that Fermi surface

undergoes reconstruction through an itinerant metamagnetic transition. We are now in the process of writing a paper for this work.

6b. Bulk spin valve effect in $\text{Ca}_3\text{Ru}_2\text{O}_7$

Spin-valve effect is first discovered in magnetic multilayered thin films by Albert Fert and Peter Grünberg who won the 2007 Nobel Prize in Physics. In spin-valve based device spins of electrons form an anti-parallel alignment between layers at zero magnetic field, but change to a parallel alignment under weak magnetic fields. Such a switch of magnetic states results in a significant decrease in electrical resistance, which is also called giant magnetoresistance effect (GMR). Our work on $\text{Ca}_3\text{Ru}_2\text{O}_7$ [5] has demonstrated that its GMR effect [6] originates from a similar spin-valve mechanism [7].

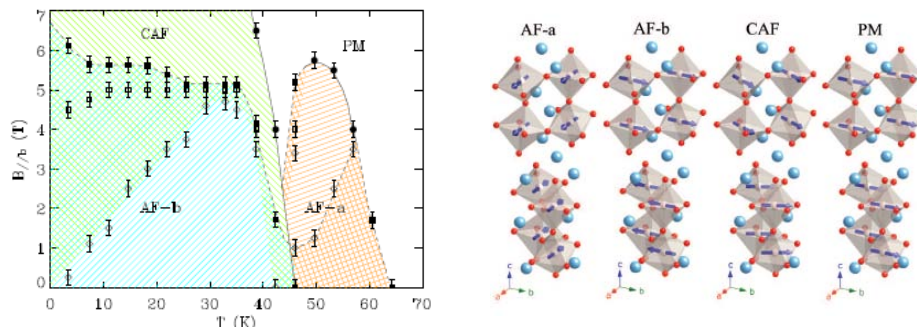


Figure 3. Left panel: Phase diagram of $\text{Ca}_3\text{Ru}_2\text{O}_7$ in a magnetic field applied along the b -axis. The solid lines denote continuous phase-transitions, and dashed lines first-order ones. The hysteresis regions are marked by cross-lines. Magnetic structures of these four phases are shown in the right panel. AF-a: antiferromagnetic phase with the easy axis along the a -axis. AF-b: antiferromagnetic phase with the easy axis along the b -axis. CAF: canted antiferromagnetic phase. PM: paramagnetic phase [5].

$\text{Ca}_3\text{Ru}_2\text{O}_7$ is an antiferromagnet with $T_N = 56\text{K}$ [8]; it has attracted a great deal of interest since it shows a GMR effect [6]. Its behavior at low temperatures is similar to that in the manganites when a magnetic field is applied perpendicular to the easy-axis of magnetization. A smaller magnetoresistive effect occurs in a first-order metamagnetic transition when the magnetic field is applied along the easy-axis. A spin-valve mechanism has been proposed in both experimental and theoretical studies for $\text{Ca}_3\text{Ru}_2\text{O}_7$ [9,7]. However, the spin-valve explanation runs into severe difficulty with the astounding experimental conclusion that the proposed fully spin-polarized phase is least favorable for electronic conduction [6]. We have solved this controversial issue through systematic neutron scattering measurements on large single crystals of $\text{Ca}_3\text{Ru}_2\text{O}_7$ in collaboration with Los Alamos National Laboratory. We have determined magnetic structures of this material under magnetic fields and established a magnetic field-temperature phase diagram, as shown in Fig. 3. The determination of these magnetic structures provides solid evidence for the bulk spin-valve mechanism for the magnetoresistivity effect of this material. The smaller magnetoresistive effect for the field applied to the easy-axis is due to the fact that the magnetic state above the transition is not a fully polarized state, but a canted antiferromagnetic state. This work was published in *Physical Review Letters* **100**, 247203 (2008). This discovery provides important clues in searching for novel materials with bulk spin valve effect, and significantly advance our understanding of GMR effect in bulk materials.

We have systematically investigated crossover magnetic states near the spin-flop transitions and the bulk spin-valve effect of $\text{Ca}_3\text{Ru}_2\text{O}_7$ through angle-resolved magnetotransport measurements. Our results reveal the magnetic states for $B//b$ to be significantly more complex than for $B//a$, as shown in the phase diagrams in Fig. 4a and 4b. When magnetic field is applied along the b -axis we probe crossover magnetic states in close proximity to phase boundaries of long-range ordered antiferromagnetic state (near T_2 in Fig. 4b) and canted antiferromagnetic state (between $T_{c0,1}$ and $T_{c0,2}$ in Fig. 4b). These crossover states are subject to the in-plane field orientation and switch to either the AFM-b state or the nearly ferromagnetic (NFM) state when the in-plane magnetic field is rotated close to the a -axis. Switching of

these magnetic states causes significant change of magnetoresistance. Moreover, we observe bulk spin valve behavior resulting from the AFM-b-to-CAFM spin-flop transition tuned by in-plane rotation of magnetic field for $B > 6\text{T}$, as shown in Fig. 4c. These results highlight the complex nature of the spin-charge coupling in $\text{Ca}_3\text{Ru}_2\text{O}_7$ and post a challenging question to the theoretical community: why does the variation of field orientation result in magnetic phase transitions? We have submitted a paper to Phys. Rev. B on this study.

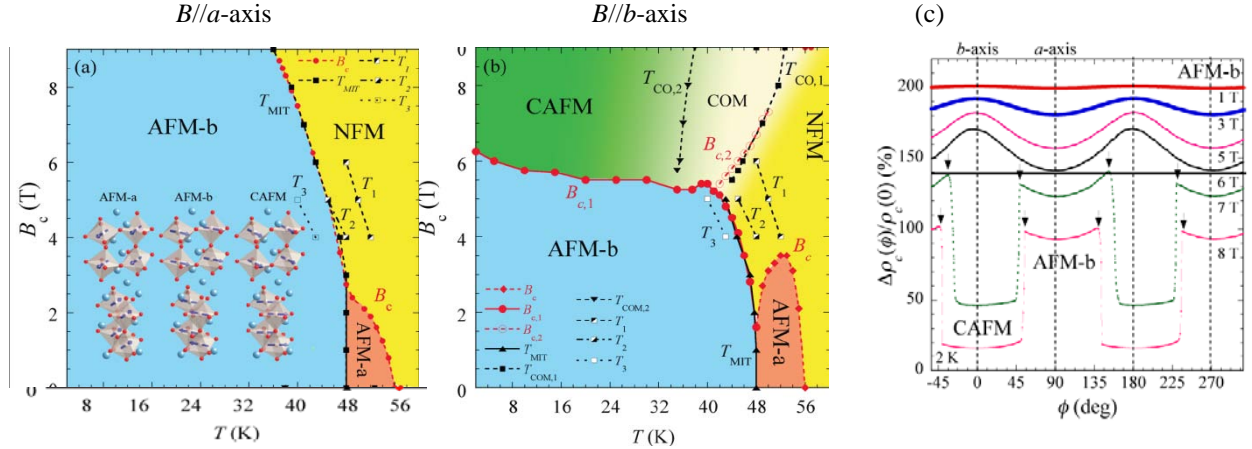


Figure 4: Magnetic phase diagram of $\text{Ca}_3\text{Ru}_2\text{O}_7$ for $B//a$ -axis (a) and $B//b$ -axis (b). AFM-a represents the AFM state with magnetic moments along the a-axis; AFM-b represents the AFM state with magnetic moments along the b-axis; CAFM represents a canted AFM state where spins in the bilayers are canted 25° from the b-axis (see Fig. 3 for these magnetic structures). NFM in both (a) and (b) denotes nearly ferromagnetic states. In close proximity to the AFM-a and AFM-b phase boundaries for $B//b$ -axis, we observe crossover magnetic (COM) states between critical temperatures $T_{co,1}$ and $T_{co,2}$ for $B > 6\text{T}$ and near T_2 for $B < 6\text{T}$. These crossover magnetic switches to either AFM-b or NFM state through an intermediate magnetic state as the in-plane magnetic field is rotated close to the a-axis. T_{MIT} in both (a) and (b) represents the metal-insulator transition temperature. (c) In-plane angle dependence of ρ_c magnetoresistivity at selected magnetic fields at 2 K. The system is in the AFM-b phase for $B \leq 6$ (top panel). When $B > 6\text{T}$ the system is in the CAFM state when field is near the b-axis and AFM-b state when field is near the a-axis. Arrows indicate the critical angles ϕ_c for spin-flop transitions. Data has been normalized and shifted for clarity.

6c. Unusual heavy-mass nearly ferromagnetic state in $(\text{Sr}_{1-x}\text{Ca}_x)_3\text{Ru}_2\text{O}_7$

We have established the magnetic phase diagram of the $(\text{Sr}_{1-x}\text{Ca}_x)_3\text{Ru}_2\text{O}_7$ solid solution series [10,11] and observed significant new phenomena in this system. We find an unusual heavy-mass nearly ferromagnetic state for $0.08 \leq x \leq 0.4$. This state exhibits a surprisingly large Wilson ratio, e.g. $R_W \sim 700$ for $x = 0.2$; it does not evolve into a long-range ferromagnetically ordered state despite extremely-strong ferromagnetic correlations, but freezes into a cluster spin glass (CG) at low temperatures. Furthermore, we observed evidence of non-Fermi liquid behavior as the spin freezing temperature approaches zero. These findings suggest that $(\text{Sr}_{1-x}\text{Ca}_x)_3\text{Ru}_2\text{O}_7$ is close to a 2D ferromagnetic state with $T_c = 0\text{K}$ [10,11]. As far as we know, such an unusual magnetic state has not been observed in any other materials. Therefore, it provides a rare opportunity to explore the novel physics of 2D ferromagnets. This work was published in *Physical Review B* **78**, 180407 (*Rapid Communication*), (2008). We have also performed systematic studies on the evolution of structure and magnetic anisotropy in $(\text{Sr}_{1-x}\text{Ca}_x)_3\text{Ru}_2\text{O}_7$. From structural refinements of x-ray diffraction spectra, we have derived structural parameters including the rotation and tilting angles of the RuO_6 octahedra, as a function of Ca content for this system. We find that the magnetic phase transitions and the magnetic anisotropy couple to the evolution of the structural distortion. The transformation from an itinerant metamagnetic state to the nearly FM state coincides with the increase in RuO_6 octahedra rotation while the transition from the nearly FM state to the AFM state coincides with the onset of RuO_6 octahedra tilting. The octahedral tilting also gives rise to magnetic anisotropy. These results indicate that the lattice and spin degrees of freedom are coupled in $(\text{Sr}_{1-x}\text{Ca}_x)_3\text{Ru}_2\text{O}_7$. This work was published in *Physical Review B* **82**, 024417 (2010).

2) Interplay between magnetism and superconductivity in the $\text{Fe}_{1+y}(\text{Te,Se})$ system

In addition to studies on ruthenates, we have expanded our research to the emerging area of Fe-based superconductors [12], focusing on the iron chalcogenide $\text{Fe}_{1+y}(\text{Te,Se})$ superconductor system. We have achieved remarkable accomplishments in this area. Immediately following Hsu *et al.*'s report of superconductivity in FeSe ($T_c \sim 8$ K) [13], we found that the T_c in this system can be enhanced up to 14 K with Te substitution for Se, and that the superconductivity of this system is close to a magnetic instability (*PRB* **78**, 224503 (2008), cited 124 times). We also determined the AFM structure of Fe_{1+y}Te (*PRL* **102**, 247001 (2009), cited 92 times), observed spin resonance below T_c (*PRL* **103**, 067008 (2009), cited 44 times), and recently established the phase diagram for $0 \leq x < 0.5$ (*Nature Materials* **9**, 716 (2010)) through collaboration with Bao, Qiu, and Broholm *et al.* These results demonstrate the unique interplay between superconductivity and magnetism in this system.

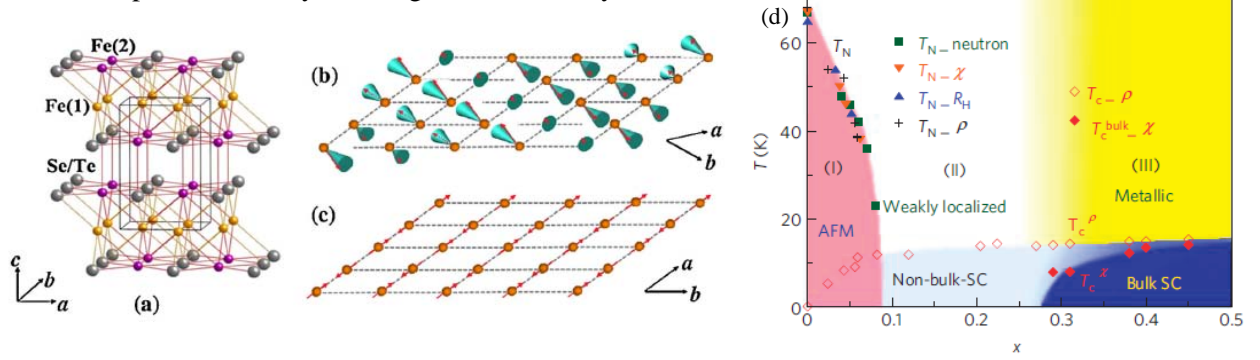


Figure 5: (a) Crystal structure of $\text{Fe}_{1+y}(\text{Te,Se})$. Magnetic structures of (b) FeTe and (c) BaFe_2As_2 are shown in the primitive Fe square lattice for comparison [14]. (d) The electronic and magnetic phase diagram of $\text{Fe}_{1.02}(\text{Te}_{1-x}\text{Se}_x)$ ($0 \leq x < 0.5$). The Néel temperature, T_N , of antiferromagnetic (AFM) phase, determined by neutron scattering (green squares), susceptibility (orange triangles), Hall coefficient (blue triangle), and resistivity (black crosses) measurements. T_c^{ρ} , onset of superconducting transition probed by resistivity (\diamond); $T_c^{\text{bulk} - \chi}$, bulk superconducting transition temperature (\blacklozenge) probed by susceptibility. Bulk superconductivity (SC) exists when sufficient Te is replaced by Se, with the superconducting volume fraction $> 75\%$ for $x \geq 0.29$. For $x < 0.29$, only non-bulk-SC exists with the superconducting volume fraction $< 3\%$ [15].

We have addressed an important issue in this system—how superconductivity with (π, π) resonance evolves from a $(\pi, 0)$ magnetic order [15]. The parent compound of this system, $\text{Fe}_{1.02}\text{Te}$, exhibits an AFM order characterized by an in-plane wave vector $\mathbf{Q}_m = (\pi, 0)$ [14], which distinguishes itself from the iron pnictide parent materials which have AFM order wavevectors of (π, π) (see Fig. 5a-5c) [16,17]. Yet both doped iron chalcogenide [18] and iron pnictide superconductors [19-21] exhibit a magnetic resonance around the same wave vector (π, π) . Resolution of the dichotomy between $(\pi, 0)$ magnetic order in FeTe and superconductivity with (π, π) magnetic resonance in optimally doped samples is a key challenge to our emerging understanding of iron based superconductivity. We have addressed this issue through systematic investigations of transport, magnetic, and superconducting properties in various regions of the phase diagram of $\text{Fe}_{1.02}(\text{Te}_{1-x}\text{Se}_x)$. We find that $(\pi, 0)$ and (π, π) magnetic correlations coexist throughout the phase diagram. The Se substitution for Te tunes the relative strength of these two magnetic correlations. Magnetic correlations of the $(\pi, 0)$ variety survive as short-range magnetic fluctuations after the long-range $(\pi, 0)$ magnetic order has been suppressed by partial Se substitution for Te. These correlations appear to suppress bulk superconductivity and lead to weak charge carrier localization in under-doped samples. Bulk superconductivity occurs only when magnetic correlations near $(\pi, 0)$ are strongly suppressed and spin fluctuations near (π, π) become dominant for $x > 0.29$, as shown in Fig.5d. These results indicate that short-range magnetic fluctuations near $(\pi, 0)$ are antagonistic to superconductivity and that the superconducting mechanisms of iron chalcogenides and iron pnictides have similar origins associated with (π, π) spin-fluctuations.

References:

- [1] M.K. Crawford, R.L. Harlow, W. Marshall, Z. Li, G. Cao, R.L. Lindstrom, Q. Huang, and J.W. Lynn, *Phys. Rev. B* **65**, 214412 (2002).
- [2] Z.Q. Mao, M. Zhou, J. Hooper, V. Golub, and C.J. O'Connor, *Phys. Rev. Lett.* **96**, 077205 (2006).
- [3] D. Fobes, M.H. Yu, M. Zhou, J. Hooper, C.J. O'Connor, M. Rosario, and Z.Q. Mao, *Phys. Rev. B* **75**, 094429 (2007).
- [4] D. Fobes, T.J. Liu, Z. Qu, M. Zhou, J. Hooper, M. Salamon, and Z. Q. Mao, *Phys. Rev. B* **81**, 172402 (2010).
- [5] Wei Bao, Z.Q. Mao, Z. Qu, J.W. Lynn, *Phys. Rev. Lett.* **100**, 247203 (2008).
- [6] X. N. Lin *et al.*, *Phys. Rev. Lett.* **95**, 017203 (2005).
- [7] D. J. Singh and S. Auluck, *Phys. Rev. Lett.* **96**, 097203 (2006).
- [8] G. Cao, S.C. McCall, and J.E. Crow, and R.P. Guertin, *Phys. Rev. B* **56**, 5387 (1997).
- [9] S. McCall *et al.* *Phys. Rev. B* **67**, 094427(2003).
- [10] Z. Qu, L. Spinu, H.Q. Yuan, V. Dobrosavljevic, W. Bao, J.W. Lynn, M. Nicklas, J. Peng, T.J. Liu, D. Fobes, E. Flesch, and Z.Q. Mao, *Phys. Rev. B* **78**, 180407 (*Rap. Com.*) (2008).
- [11] Zhe Qu, Jin Peng, Tijiang Liu, David Fobes, Leonard Spinu, and Zhiqiang Mao, *Phys. Rev. B* **80**, 115130 (2009).
- [12] J. Paglione and R.L. Greene, *Nature Physics* **6**, 645 (2010).
- [13] F. C. Hsu *et al.*, *Proc. Natl. Acad. Sci. U.S.A.* **105**, 14262 (2008).
- [14] W. Bao, Y. Qiu, Q. Huang, M. A. Green, P. Zajdel, M. R. Fitzsimmons, M. Zhernenkov, S. Chang, M. Fang, B. Qian, E. K. Vehstedt, J. Yang, H. M. Pham, L. Spinu, and Z. Q. Mao, *Phys. Rev. Lett* **102**, 247001 (2009).
- [15] T. J. Liu, J. Hu, B. Qian, D. Fobes, Z. Q. Mao, W. Bao, M. Reehuis, S. A. J. Kimber, K. Prokeš, S. Matas, D. N. Argyriou, A. Hiess, A. Rotaru, H. Pham, L. Spinu, Y. Qiu, V. Thampy, A. T. Savici, J. A. Rodriguez, and C. Broholm, *Nat. Mater.* **9**, 718 (2010).
- [16] C. de la Cruz, Q. Huang, J. W. Lynn, J. Li, W. R. Li, J. L. Zarestky, H. A. Mook, G. F. Chen, J. L. Luo, N. L. Wang, and P. Dai, *Nature* **453**, 899 (2008).
- [17] Q. Huang, Y. Qiu, W. Bao, M. A. Green, J. W. Lynn, Y. C. Gasparovic, T. Wu, G. Wu, and X. H. Chen, *Phys. Rev. Lett* **101**, 257003 (2008).
- [18] Y. Qiu, W. Bao, Y. Zhao, C. Broholm, V. Stanev, Z. Tesanovic, Y. C. Gasparovic, S. Chang, J. Hu, B. Qian, M. Fang, and Z. Mao, *Phys. Rev. Lett* **103**, 067008 (2009)
- [19] A. D. Christianson *et al.* *Nature* **456**, 930 (2008).
- [20] M. D. Lumsden *et al.*, *Phys. Rev. Lett.* **102**, 107005 (2009).
- [21] S. Chi *et al.*, *Phys. Rev. Lett.* **102**, 107006 (2009).

7. List of papers or patents (already published, in press, submitted) in which DOE support is acknowledged.

- *Magnetic, electrical transport, and thermoelectric properties of $Sr_4Ru_3O_{10}$: Evidence for a field-induced electronic phase transition at low temperatures,*
Z.A. Xu, X.F. Xu, R. S. Freitas, Z.Y. Long, M. Zhou, D. Fobes, M.F. Fang, P. Schiffer, Z.Q. Mao, and Y. Liu, *Phys. Rev. B* **76**, 094405, (2007)
- Spin-valve effect and magnetoresistivity in single crystalline $Ca_3Ru_2O_7$
Wei Bao, Z.Q. Mao, Z. Qu, J.W. Lynn
Phys. Rev. Lett. **100**, 247203 (2008).
- Band-dependent normal-state coherence in Sr_2RuO_4 : Evidence from Nerst and thermopower measurements,
X.F. Xu, Z.A. Xu, T.J. Liu, D. Fobes, Z.Q. Mao, J.L. Luo, and Y. Liu,
Phys. Rev. Lett. **101**, 057002 (2008).
- *Unusual heavy-mass nearly ferromagnetic state with a surprisingly large Wilson ratio in the double layered ruthenates $(Sr_{1-x}Ca_x)_3Ru_2O_7$,*
Z. Qu, L. Spinu, H.Q. Yuan, V. Dobrosavljevic, W. Bao, J.W. Lynn, M. Nicklas, J. Peng, T.J. Liu, D. Fobes, E. Flesch, and Z.Q. Mao,
Phys. Rev. B **78**, 180407 (Rapid Communications) (2008).
- *Superconductivity close to magnetic instability in $Fe(Se_{1-x}Te_x)_{0.82}$*
M.H. Fang, H.M. Pham, B. Qian, T.J. Liu, E.K. Vehstedt, Y. Liu, L. Spinu, and Z.Q. Mao,
Phys. Rev. B **78**, 224503 (2008) (Editor's suggestion).
- *Suppression of Proximity Effect and the Enhancement of p-Wave Superconductivity in the Sr_2RuO_4 -Ru System,*
Y.A. Ying, Y. Xin Y, B.W. Clouser, E. Hao, N.E. Staley, R.J. Myers RJ, L.F. Allard, D. Fobes D, T.J. Liu, Z.Q. Mao, and Y. Liu, *Phys. Rev. Lett.* **103**, 247004 (2009).
- *Magnetic, magnetocaloric and magnetoresistance properties of Nd_7Pd_3 ,*
N.K. Singh, P. Kumar, Z.Q. Mao, D. Paudyal, V. Neu, K.G. Suresh, V.K. Pecharsky, K.A. Gschneidner, *J. Phys. C* **21**, 456004 (2009).
- *Charge-carrier localization induced by excess Fe in the superconductor $Fe_{1+y}Te_{1-x}Se_x$,*
T.J. Liu, X. Ke, B. Qian, J. Hu, D. Fobes, E.K. Vehstedt, H. Pham, J. H. Yang, M.H. Fang, L. Spniu, P. Schiffer, Y. Liu, and Z.Q. Mao, *Phys. Rev. B* **80**, 174509 (2009).
- *Complex electronic states in double layered ruthenates $(Sr_{1-x}Ca_x)_3Ru_2O_7$,*
Zhe Qu, Jin Peng, Tijiang Liu, David Fobes, Leonard Spinu, and Z.Q. Mao,
Phys. Rev. B **80**, 115130 (2009).
- *Spin gap and resonance at the nesting wavevector in superconducting $FeSe_{0.4}Te_{0.6}$,*
Y.M. Qiu, W. Bao, Y. Zhao, C. Broholm, V. Stanev, Z. Tesanovic, Y.C. Gasparovic, S. Chang, J. Hu, B. Qian, M.H. Fang, and Z.Q. Mao, *Phys. Rev. Lett.* **103**, 067008 (2009).

- *Tunable ($\delta\pi, \delta\pi$)-type antiferromagnetic order in α -Fe(Te,Se) superconductor,*
W. Bao, Y. Qiu, Q. Huang, M.A. Green, P. Zajdel, M.R. Fitzsimmons, M. Zhernenkov, M.H. Fang, B. Qian, E.K. Vehstedt, J.H. Yang, H.M. Pham, L. Spinu, and Z.Q. Mao, *Phys. Rev. Lett.* **102**, 247001 (2009).
- *Real-space observation of magnetic domain structure at metamagnetic transition in a triple-layer ruthenate $Sr_4Ru_3O_{10}$,*
Y Nakajima, Y Matsumoto, D. Fobes, M. Zhou, Z.Q. Mao and T. Tamegai, *J. Phys.: Conf. Ser.* **150**, 042134 (2009).
- *Structural, magnetic, and electronic transport properties of $(Sr_{0.9}Ca_{0.1})_3Ru_2O_7$ single crystal,*
Bin Qian, Zhe Qu, Jin Peng, Tijiang Liu, Xiaoshan Wu, L. Spinu, and Z.Q. Mao, *J. Appl. Phys.* **105**, 07E323 (2009).
- *Interplay between the lattice and spin degrees of freedom in $(Sr_{1-x}Ca_x)_3Ru_2O_7$,*
J. Peng, Z. Qu, B. Qian, D. Fobes, T.J. Liu, X.S. Wu, H.M. Pham, L. Spinu, and Z.Q. Mao, *Phys. Rev. B* **82**, 024417 (2010).
- *Anisotropy of magnetoresistivities in $Sr_4Ru_3O_{10}$: Evidence for an orbital-selective metamagnetic transition,*
D. Fobes, T.J. Liu, Z. Qu, M. Zhou, J. Hooper, M. Salamon, and Z. Q. Mao, *Phys. Rev. B* **81**, 172402 (2010).
- *From $(\pi, 0)$ magnetic order to superconductivity with (π, π) magnetic resonance in $Fe_{1.02}(Te_{1-x}Se_x)$,*
T.J. Liu, J. Hu, B. Qian, D. Fobes, Z.Q. Mao, W. Bao, M. Reehuis, S.A.J. Kimber, K. Prokes, S. Matas, D.N. Argyriou, A. Hiess, A. Rotaru, H. Pham, L. Spinu, Y. Qiu, V. Thampy, A.T. Savici, J. A. Rodriguez, and C. Broholm, *Nature materials* **9**, 716 (2010).
- *Incommensurate itinerant antiferromagnetic excitations and spin resonance in the $FeTe_{0.6}Se_{0.4}$ superconductor,*
D. N. Argyriou, A. Hiess, A. Akbari, I. Eremin, M.M. Korshunov, J. Hu, B. Qian, Z.Q. Mao, Y.M. Qiu, C. Broholm, and W. Bao, *Phys. Rev. B* **81**, 220503 (2010).
- *Doping and dimensionality effects on the core-level spectra of layered ruthenates,*
H.Z. Guo, Y. Li, D. Urbina, B. Hu, R.Y. Jin, T.J. Liu, D. Fobes, Z.Q. Mao, E. W. Plummer, J.D. Zhang, *Phys. Rev. B* **81**, 155121 (2010).
- *Calorimetric Evidence of Strong-Coupling Multiband Superconductivity in $Fe(Te_{0.57}Se_{0.43})$ Single Crystal,*
J. Hu, T.J. Liu, B. Qian, A. Rotaru, L. Spinu, and Z.Q. Mao, to appear in *Phys. Rev. B*.
- *Metastable magnetic states and the bulk spin valve effect in $Ca_3Ru_2O_7$*
D. Fobes, J. Peng, Z. Qu, T. J. Liu, and Z. Q. Mao, submitted to *Phys. Rev. B*.
- *A triplet Resonance in Superconducting $FeSe_{0.4}Te_{0.6}$,*
Wei Bao, A. T. Savici, G. E. Granroth, C. Broholm, K. Habicht, Y. Qiu, Jin Hu,

T.J. Liu, and Z.Q. Mao, *submitted to Phys. Rev. Lett.* [arXiv:1002.1617](https://arxiv.org/abs/1002.1617)

8. A total list of people who worked on the project

Zhiqiang Mao, Principal Investigator, directing this project, receiving one-month summer salary support.
Zhe Qu, postdoc scholar, fully supported by this project from Jan.1 to Aug.15, 08, working on the $(\text{Sr}_{1-x}\text{Ca}_x)_3\text{Ru}_2\text{O}_7$ project.

Pramod Kumar, postdoc scholar, fully supported by this project from Feb. 2009 to Feb. 2010, working on the $\text{Sr}_4\text{Ru}_3\text{O}_{10}$ project.

Tijiang Liu, graduate student, fully supported by this project from May 2007 to Aug. 2010, working on $\text{Sr}_4\text{Ru}_3\text{O}_{10}$ and Fe-based superconductors.

David Fobes, graduate student, partially supported by this project (10%), performing magneto transport studies on $\text{Sr}_4\text{Ru}_3\text{O}_{10}$ and $\text{Ca}_3\text{Ru}_2\text{O}_7$.

Jin Peng, graduate student, partially supported by this project (20%), crystal growth and structure characterization of $(\text{Sr}_{1-x}\text{Ca}_x)_3\text{Ru}_2\text{O}_7$.

Erin K Vehstedt, undergraduate student, partially supported by this project (25%), focusing on crystal growth of ruthenates.

9. An updated list of other support (current and pending, federal and non-federal.)

NSF CAREER: New Physical Phenomena in Ruthenate Materials, **current**,

NSF, \$ 410,000, single PI, 06/01/2007- 05/30/2012, one month summer salary.

This project focuses on studying new physical phenomena of strongly correlated ruthenates with various structures, including perovskites $(\text{Sr}_{1-x}\text{Ca}_x)_3\text{Ru}_2\text{O}_7$, quasi-one-dimensional hollandite $\text{BaRu}_6\text{O}_{12}$, and cubic $\text{La}_4\text{Ru}_6\text{O}_{19}$. The goal and approach of this project differ from those of the DOE project.

DOD (EPSCoR program), 9/15/09-9/16/2012, \$450,000, **current**,

“*Study of metal-insulator transitions of calcium ruthenates for bolometric detection*” (Lead P.I., together with Ulrike Diebold and Daeho kim at Tulane, and Leonard Spinu at University to New Orleans). 0.64 month summer salary for the 2nd and 3rd year. This project aims at exploring potential application of metal-insulator transitions of calcium ruthenates in bolometric detection (Tulane), no overlap with the DOE project.

Preserving half-metallicity on the surface of Fe_3O_4 for spintronic applications

Louisiana Board of Regents (Industrial Ties Subprogram), \$226,149 (\$112,500 to Tulane), co-PI, together with Jinke Tang (University of New Orleans) and Ulrike Diebold (Tulane), 06/01/ 2007 – 05/31/2011, no summer salary, no overlap with the DOE project.

NSF EPSCoR/Louisiana Board of Regents (57 Co-PIs), Louisiana Alliance for Simulation-Guided Materials Applications, \$2,752,914 to Tulane (one of 10 Co-PIs at Tulane), **current**, 2010-2015, 0.7 month summer salary, no overlap with the DOE project.

Louisiana Board of Regents, traditional enhancement program, \$222,790, **approved for funding**,

An ion milling system to enhance research and education in material science and engineering at Tulane (Lead PI: Zhiqiang Mao, Co-PI: Dae Ho Kim, Brent D Koplitz, and Noshir Pesika at Tulane University) 07/01/2011-06/30/2012.

DOE, 6/1/2011-5/31/14, total requested amount \$462,032, **pending**

“*Study of magnetism and superconductivity of iron chalcogenide $Fe_{1+y}(Te_{1-x}Se_x)$* ” (Single P.I.), requesting one-month summer salary for each project year. The DOE-EPSCoR project helped the PI expand into this emerging area.

10. Cost status:

10.1. Approved budget for the full budget period

	Year 1	Year 2	Year 3	Total
Mao-1 month summer	6,890	7,097	7,310	21,297
Postdoc scholar	36,000	36,000	36,000	108,000
Graduate Student	24,000	24,000	24,000	72,000
Undergraduate	3,000	3,000	3,000	9,000
Fringe Benefits	11,683	11,696	11,709	35,088
Travel	5,000	5,000	5,000	15,000
Supplies	13,098	12,878	12,652	38,628
Publications	1,000	1,000	1,000	3,000
Total direct	100,671	100,671	100,671	302,013
Indirect (49% MTDC)	49,329	49,329	49,329	147,987
Total costs	150,000	150,000	150,000	\$ 450,000

TULANE MATCHING FUNDS: \$68,034

	Year 1	Year 2	Year 3	Total
Undergraduate	8,726	8,726	8,726	26,178
Fringe Benefits	454	454	454	1,362
Equipment	9,000	9,000	9,000	27,000
Indirect cost	4,498	4,498	4,498	13,494
Total Tulane matching budget	22,678	22,678	22,678	\$ 68,034

10.2 Actual costs incurred

	DOE grant	Tulane match
Mao-1 month summer for each project year	26,801.77	
Postdoc scholar	74,621.90	
Graduate Student	79,876.45	
Undergraduate student	2,506.25	
Fringe Benefits	24,478.50	
Travel	19,069.82	
Supplies + minor equipment	74,848.05	10,787.87
Equipment		51,308.49
Indirect (49% MTDC)	148,079.40	5,286.06
Total:	\$450,282.14	\$ 67,382.42